Diffraction at HERA

Laurent Schoeffel
CE Saclay
Irfu/SPP
F-91191 Gif-sur-Yvette Cedex, FRANCE

1 Introduction

Between 1992 and 2007, the HERA accelerator provided *ep* collisions at center of mass energies beyond 300 GeV at the interaction points of the H1 and ZEUS experiments. Perhaps the most interesting results to emerge relate to the newly accessed field of perturbative strong interaction physics at low Bjorken-x, where parton densities become extremely large. Questions arise as to how and where non-linear dynamics tame the parton density growth [1] and challenging features such as geometric scaling [2] are observed. Central to this low x physics landscape is a high rate of diffractive processes, in which a colorless exchange takes place and the proton remains intact. In particular, the study of semi-inclusive diffractive deep-inelastic scattering (DDIS), $\gamma^* p \to Xp$ [3, 4] has led to a revolution in our microscopic, parton level, understanding of the structure of elastic and quasi-elastic high energy hadronic scattering. Comparisons with hard diffraction in proton-(anti)proton scattering have also improved our knowledge of absorptive and underlying event effects in which the diffractive signature may be obscured by multiple interactions in the same event [5]. In addition to their fundamental interest in their own right, these issues are highly relevant to the modeling of chromodynamics at the LHC [6].

The kinematic variables describing DDIS are illustrated in Fig.1a. The longitudinal momentum fractions of the colorless exchange with respect to the incoming proton and of the struck quark with respect to the colorless exchange are denoted $x_{I\!P}$ and β, respectively, such that $\beta\, x_{I\!P} = x$. The squared four-momentum transferred at the proton vertex is given by the Mandelstam t variable. The semi-inclusive DDIS cross section is usually presented in the form of a diffractive reduced cross section $\sigma_r^{D(3)}$, integrated over t and related to the experimentally measured differential cross section by [7]

$$\frac{\mathrm{d}^3\sigma^{ep\to eXp}}{\mathrm{d}x_{I\!P}\ \mathrm{d}x\ \mathrm{d}Q^2} = \frac{2\pi\alpha^2}{xQ^4}\cdot Y_+ \cdot \sigma_r^{D(3)}(x_{I\!P}, x, Q^2)\ , \tag{1}$$

where $Y_+ = 1 + (1-y)^2$ and y is the usual Bjorken variable. The reduced cross section depends at moderate scales, Q^2, on two diffractive structure functions $F_2^{D(3)}$

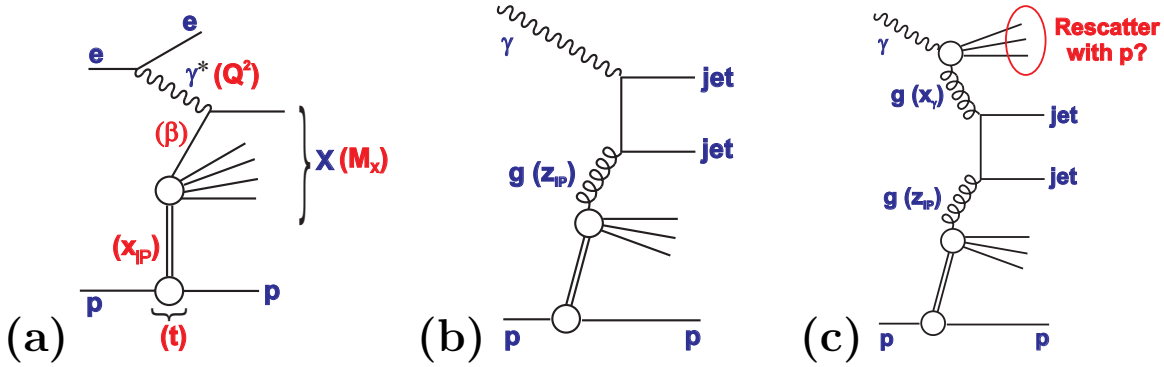

Figure 1: Sketches of diffractive ep processes. (a) Inclusive DDIS at the level of the quark parton model, illustrating the kinematic variables discussed in the text. (b) Dominant leading order diagram for hard scattering in DDIS or direct photoproduction, in which a parton of momentum fraction $z_{I\!P}$ from the DPDFs enters the hard scattering. (c) A leading order process in resolved photoproduction involving a parton of momentum fraction x_γ relative to the photon.

and $F_L^{D(3)}$ according to

$$\sigma_r^{D(3)} = F_2^{D(3)} - \frac{y^2}{Y_+} F_L^{D(3)}. \tag{2}$$

For y not too close to unity, $\sigma_r^{D(3)} = F_2^{D(3)}$ holds to very good approximation.

2 Measurement methods and comparisons

Experimentally, diffractive ep scattering is characterized by the presence of a leading proton in the final state, retaining most of the initial state proton energy, and by a lack of hadronic activity in the forward (outgoing proton) direction, such that the system X is cleanly separated and its mass M_X may be measured in the central detector components. These signatures have been widely exploited at HERA to select diffractive events by tagging the outgoing proton in the H1 Forward Proton Spectrometer or the ZEUS Leading Proton Spectrometer ('LPS method' [8, 9, 10]) or by requiring the presence of a large gap in the rapidity distribution of hadronic final state particles in the forward region ('LRG method' [7, 9, 11]). In a third approach, not considered in detail here, the inclusive DIS sample is decomposed into diffractive and non-diffractive contributions based on their characteristic dependences on M_X [11, 12]. Whilst the LRG and M_X-based techniques yield better statistics than the LPS method, they suffer from systematic uncertainties associated with an admixture of proton dissociation to low mass states, which is irreducible due to the limited forward detector acceptance.

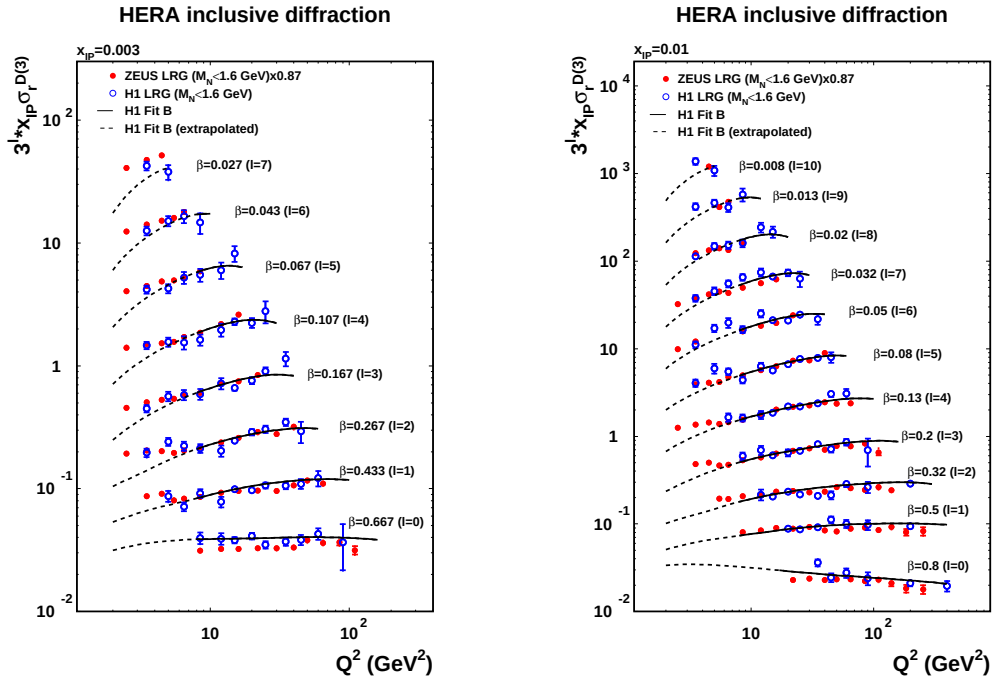

Figure 2: H1 and ZEUS measurements of the diffractive reduced cross section at two example $x_{I\!P}$ values [13]. The ZEUS data are scaled by a factor of 0.87 to match the H1 normalisation. The data are compared with the results of the H1 2006 Fit B DPDF based parameterization [7] for $Q^2 \geq 8.5$ GeV^2 and with its DGLAP (QCD) based extrapolation to lower Q^2.

The H1 collaboration recently released a preliminary proton-tagged measurement using its full available FPS sample at HERA-II [10]. The integrated luminosity is 156 pb^{-1}, a factor of 20 beyond previous H1 measurements. The new data tend to lie slightly above the recently published final ZEUS LPS data from HERA-I [9], but are within the combined normalization uncertainty of around 10%. The most precise test of compatibility between H1 and ZEUS is obtained from the LRG data. The recently published ZEUS data [9] are based on an integrated luminosity of 62 pb^{-1} and thus have substantially improved statistical precision compared with the older H1 published results [7]. The normalization differences between the two experiments are most obvious here, having been quantified at 13%, which is a little beyond one standard deviation in the combined normalization uncertainty. After correcting for this factor, very good agreement is observed between the shapes of the H1 and ZEUS cross sections throughout most of the phase space studied, as shown in Fig. 2. A more detailed comparison between different diffractive cross section measurements by H1 and ZEUS and a first attempt to combine the results of the two experiments can

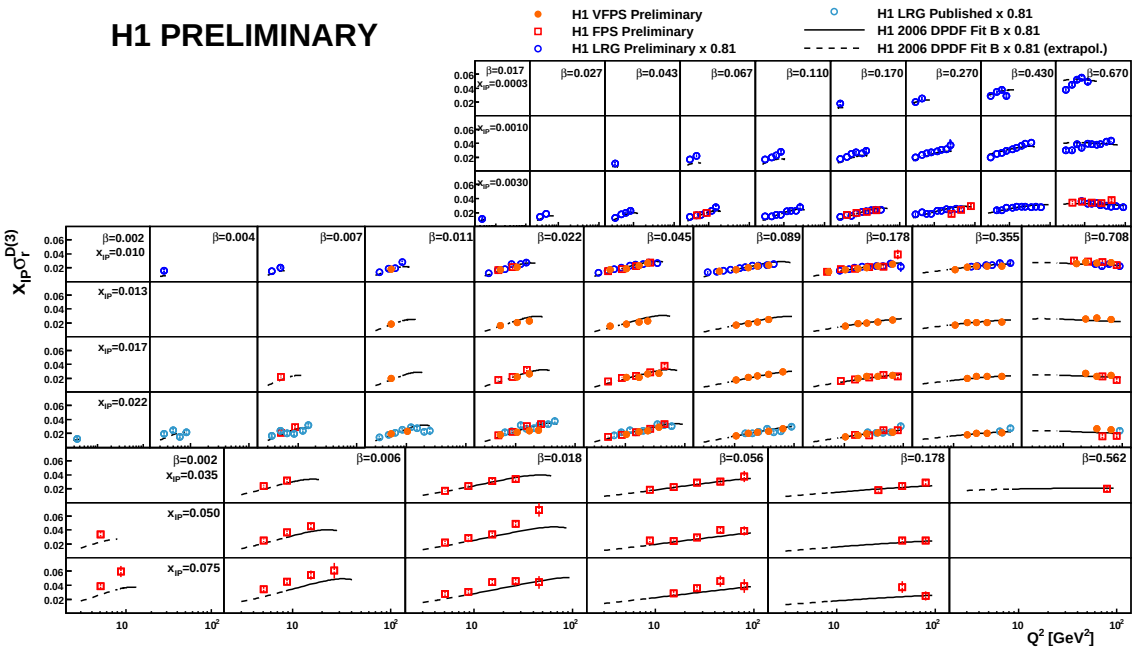

Figure 3: H1 measurements of the diffractive reduced cross section. The Q^2 dependence is shown at numerous β and $x_{I\!P}$ values.

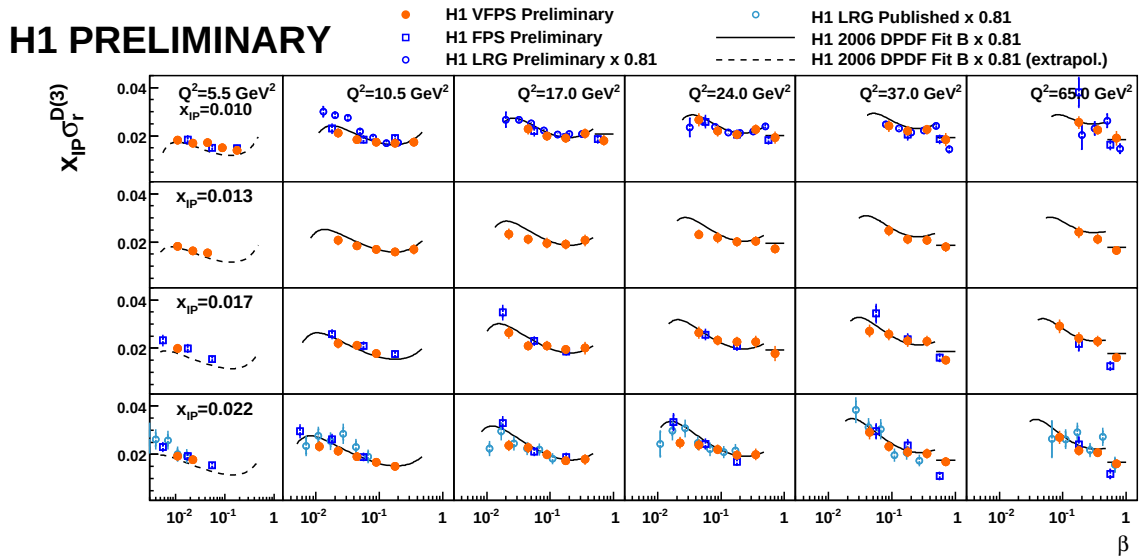

Figure 4: H1 measurements of the diffractive reduced cross section. The β dependence is shown at numerous Q^2 and $x_{I\!P}$ values.

be found in [13]. Fig. 3 and 4 present a complete summary of various measurements of the H1 experiment (using different experimental methods).

3 Soft physics at the proton vertex

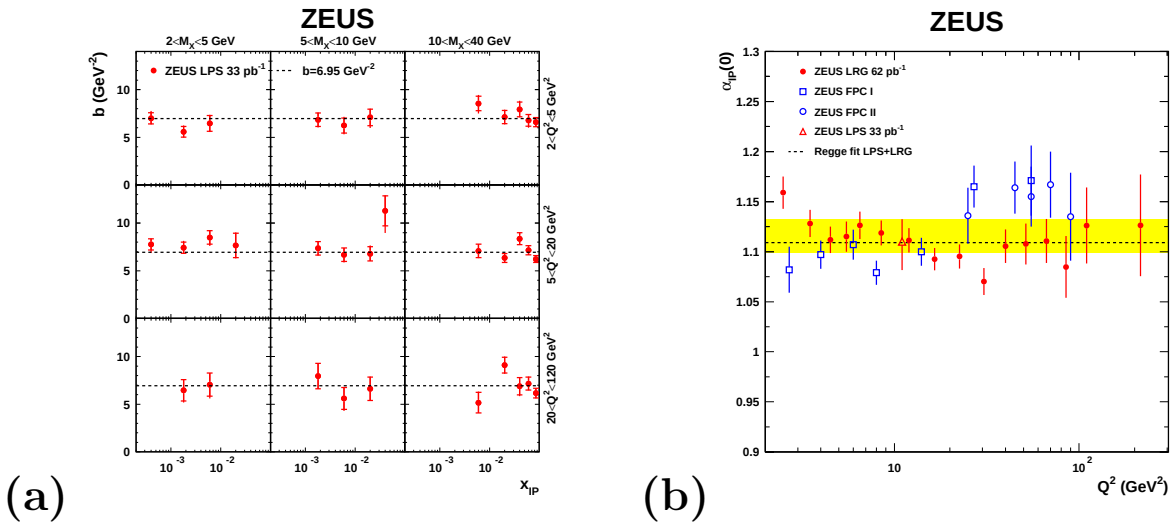

Figure 5: a) Measurements of the exponential t slope from ZEUS LPS data, shown as a function of Q^2, $x_{I\!P}$ and M_X. b) ZEUS extractions of the effective pomeron intercept describing the $x_{I\!P}$ dependence of DDIS data at different Q^2 values [9].

To good approximation, LRG and LPS data show [7, 8, 9] that DDIS data satisfy a proton vertex factorization, whereby the dependences on variables which describe the scattered proton ($x_{I\!P}$, t) factorise from those describing the hard partonic interaction (Q^2, β). For example, the slope parameter b, extracted in [9] by fitting the t distribution to the form $\mathrm{d}\sigma/\mathrm{d}t \propto e^{bt}$, is shown as a function of DDIS kinematic variables in Fig. 5a. There are no significant variations from the average value of $b \simeq 7$ GeV^{-2} anywhere in the studied range. The measured value of b is significantly larger than that from 'hard' exclusive vector meson production ($ep \to eVp$). It is characteristic of an interaction region of spatial extent considerably larger than the proton radius, indicating that the dominant feature of DDIS is the probing with the virtual photon of non-perturbative exchanges similar to the pomeron of soft hadronic physics [16].

Fig. 5b shows the Q^2 dependence of the effective pomeron intercept $\alpha_{I\!P}(0)$, which is extracted from the $x_{I\!P}$ dependence of the data [9]. No significant dependence on Q^2 is observed, again compatible with proton vertex factorization. These results are consistent with the H1 value of $\alpha_{I\!P}(0) = 1.118 \pm 0.008$ (exp.) $^{+0.029}_{-0.010}$ (model) [7].

Both collaborations have also extracted a value for the slope of the effective pomeron trajectory, the recently published ZEUS value being $\alpha'_{I\!P} = -0.01 \pm 0.06$ (stat.) $\pm$ 0.06 (syst.) GeV^{-2} [9].

The intercept of the effective pomeron trajectory is consistent within errors with the 'soft pomeron' results from fits to total cross sections and soft diffractive data [17]. Although larger effective intercepts have been measured in hard vector meson production, no deviations with either Q^2 or β have yet been observed in inclusive DDIS. The measured slope of the effective trajectory is smaller than the canonical soft diffractive value of 0.25 GeV^{-2} [18], though it is compatible with results from the soft exclusive photoproduction of ρ^0 mesons at HERA [19].

4 Diffractive Parton Density Functions

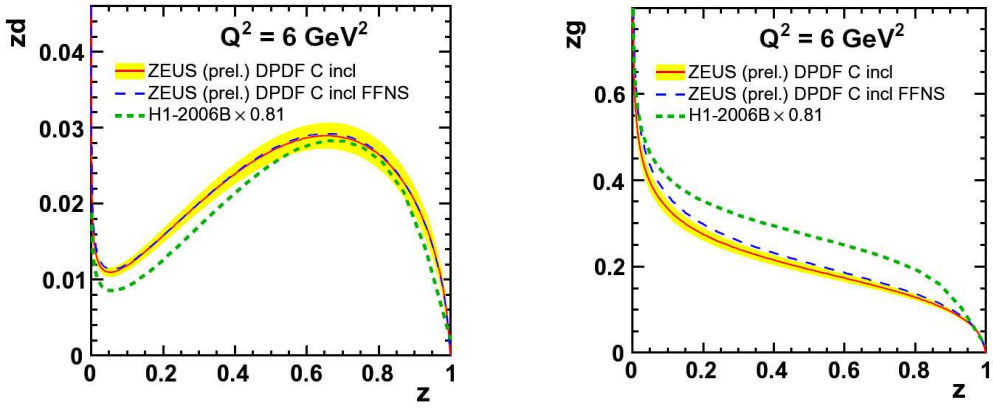

Figure 6: ZEUS down quark (one sixth of the total quark + antiquark) and gluon densities as a function of generalized momentum fraction z at $Q^2 = 6$ GeV^2 [23]. Two heavy flavor schemes are shown, as well as H1 results [7] corrected for proton dissociation with a factor of 0.81.

In the framework of the proof [20] of a hard scattering collinear QCD factorisation theorem for semi-inclusive DIS processes such as DDIS, the concept of 'diffractive parton distribution functions' (DPDFs) [21] may be introduced, representing conditional proton parton probability distributions under the constraint of a leading final state proton with a particular four-momentum.

The differential DDIS cross section may then be written in terms of convolutions of partonic cross sections $\hat{\sigma}^{ei}(x, Q^2)$ with DPDFs f_i^D as

$$\mathrm{d}\sigma^{ep\to eXp}(x, Q^2, x_{I\!P}, t) = \sum_i f_i^D(x, Q^2, x_{I\!P}, t) \otimes \mathrm{d}\hat{\sigma}^{ei}(x, Q^2) \,. \qquad (3)$$

The empirically motivated proton vertex factorization property (section 3) suggests a further factorization, whereby the DPDFs vary only in normalization with the four-momentum of the final state proton as described by $x_{I\!P}$ and t:

$$f_i^D(x, Q^2, x_{I\!P}, t) = f_{I\!P/p}(x_{I\!P}, t) \cdot f_i(\beta = x/x_{I\!P}, Q^2) \ . \tag{4}$$

Parameterizing $f_{I\!P/p}(x_{I\!P}, t)$ using Regge asymptotics, equation 4 amounts to a description of DDIS in terms of the exchange of a factorisable pomeron with universal parton densities [22]. The β and Q^2 dependences of σ_r^D may then be subjected to a perturbative QCD analysis based on the DGLAP equations in order to obtain DPDFs. Whilst F_2^D directly measures the quark density, the gluon density is only indirectly constrained, via the scaling violations $\partial F_2^D / \partial \ln Q^2$.

The high statistics ZEUS LRG and LPS data [9] have recently been fitted to extract DPDFs [23]. The method and DPDF parameterization are similar to an earlier H1 analysis [7], the main step forward being in the heavy flavor treatment, which now follows the general mass variable flavor number scheme [24]. In Fig. 6, the resulting DPDFs are compared with results from both ZEUS and H1 using a fixed flavor number scheme. The agreement between the experiments is reasonable when the uncertainty on the H1 DPDFs is also taken into account and the conclusion that the dominant feature is a gluon density with a relatively hard z dependence is confirmed. The error bands shown in Fig. 6 represent experimental uncertainties only. Whilst the quark densities are rather well known throughout the phase space, the theoretical uncertainties on the gluon density are large. Indeed, in the large z region, where the dominant parton splitting is $q \to qg$, the sensitivity of $\partial F_2^D / \partial \ln Q^2$ to the gluon density becomes poor and different DPDF parameterizations lead to large variations [7, 23]. Improved large z constraints have been obtained by including dijet data in the QCD fits [25, 23].

In common with the inclusive proton PDFs at low x, the DPDFs exhibit a ratio of around 7:3 between gluons and quarks, consistent with a common QCD radiation pattern far from the valence region.

5 Nucleon tomography

Measurements of the DIS (or DDIS) of leptons and nucleons, $e + p \to e + X$ (or $e + p \to e + X + Y$), allow the extraction of Parton Distribution Functions (PDFs) (or diffractive PDFs) which describe the longitudinal momentum carried by the quarks, anti-quarks and gluons that make up the fast-moving nucleons. While PDFs provide crucial input to perturbative QCD calculations of processes involving hadrons, they do not provide a complete picture of the partonic structure of nucleons [26]. In particular, PDFs contain neither information on the correlations between partons nor on their transverse motion. Hard exclusive processes, in which the nucleon remains intact,

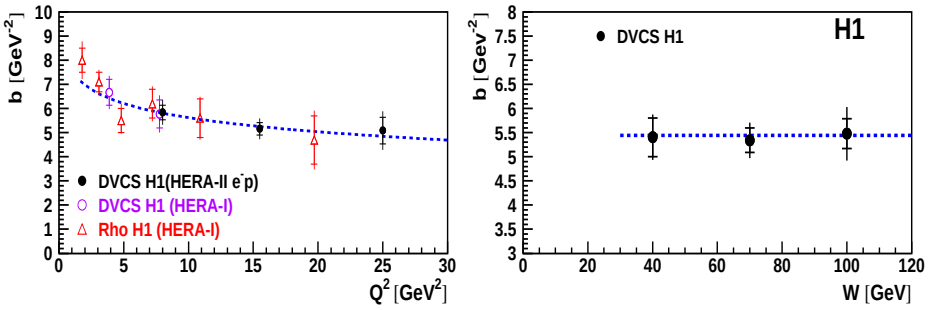

Figure 7: The logarithmic slope of the t dependence for DVCS and ρ exclusive production : $d\sigma/dt \propto \exp(-b|t|)$ where $t = (p - p')^2$.

have emerged in recent years as prime candidates to complement this essentially one dimensional picture. The simplest exclusive process is the deeply virtual Compton scattering (DVCS) or exclusive production of real photon, $e + p \to e + \gamma + p$. This process is of particular interest as it has both a clear experimental signature and is calculable in perturbative QCD. The DVCS reaction can be regarded as the elastic scattering of the virtual photon off the proton via a colorless exchange, producing a real photon in the final state [27, 28]. In the Bjorken scaling regime, QCD calculations assume that the exchange involves two partons, having different longitudinal and transverse momenta, in a colorless configuration. These unequal momenta or skewing are a consequence of the mass difference between the incoming virtual photon and the outgoing real photon. This skewness effect can be interpreted in the context of generalized parton distributions (GPDs) [29] and can bring new insights on the quarks/gluons imaging of the nucleon.

One of the key measurement in exclusive processes is the slope defined by the exponential fit to the differential cross section: $d\sigma/dt \propto \exp(-b|t|)$ at small t, where $t = (p-p')^2$ is the square of the momentum transfer at the proton vertex (see Fig. 7). A Fourier transform from momentum to impact parameter space readily shows that the t-slope b is related to the typical transverse distance between the colliding objects [30, 31]. At high scale, the $q\overline{q}$ dipole is almost point-like, and the t dependence of the cross section is given by the transverse extension of the gluons (or sea quarks) in the proton for a given x_{Bj} range. More precisely, from the generalized gluon distribution F_g defined in section 3, we can compute a gluon density which also depends on a spatial degree of freedom, the transverse size (or impact parameter), labeled $R_\perp$, in the proton. Both functions are related by a Fourier transform

$$g(x, R_\perp; Q^2) \equiv \int \frac{d^2\Delta_\perp}{(2\pi)^2} \exp[i(\Delta_\perp R_\perp)]\, F_g(x, t = -\Delta_\perp^2; Q^2).$$

Thus, the transverse extension $\langle r_T^2 \rangle$ of gluons (or sea quarks) in the proton can be

written as

$$\langle r_T^2 \rangle \equiv \frac{\int d^2R_\perp \, g(x,R_\perp) \, R_\perp^2}{\int d^2R_\perp \, g(x,R_\perp)} = 4 \frac{\partial}{\partial t} \left[\frac{F_g(x,t)}{F_g(x,0)} \right]_{t=0} = 2b$$

where b is the exponential t-slope. Measurements of b have been performed for different channels, as DVCS or ρ production (see Fig. 7-left-), which corresponds to $\sqrt{r_T^2} = 0.65 \pm 0.02$ fm at large scale Q^2 for $x_{Bj} \simeq 10^{-3}$. This value is smaller that the size of a single proton, and, in contrast to hadron-hadron scattering, it does not expand as energy W increases (see Fig. 7-right-). This result is consistent with perturbative QCD calculations in terms of a radiation cloud of gluons and quarks emitted around the incoming virtual photon.

5.1 Link with LHC issues

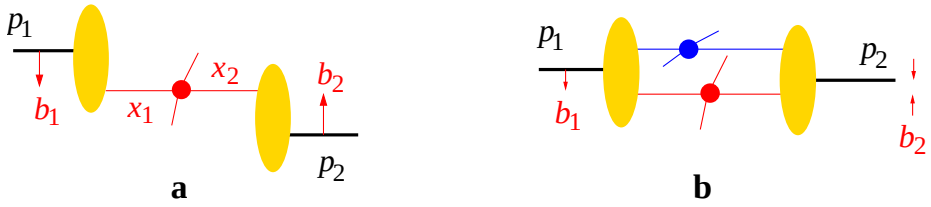

Figure 8: a: Graph with a single hard interaction in a hadron-hadron collision. The impact parameters b_1 and b_2 are integrated over independently. b: Graph with a primary and a secondary interaction.

The correlation between the transverse distribution of partons and their momentum fraction is not only interesting from the perspective of hadron structure, but also has practical consequences for high-energy hadron-hadron collisions. Consider the production of a high-mass system (a dijet or a heavy particle). For the inclusive production cross section, the distribution of the colliding partons in impact parameter is not important: only the parton distributions integrated over impact parameters are relevant according to standard hard-scattering factorization (see Fig. 8(a)). There can however be additional interactions in the same collision, especially at the high energies for the Tevatron or the LHC, as shown in Fig. 8(b). Their effects cancel in sufficiently inclusive observables, but it does affect the event characteristics and can hence be quite relevant in practice. In this case, the impact parameter distribution of partons must be considered.

The production of a heavy system requires large momentum fractions for the colliding partons. A narrow impact parameter distribution for these partons forces the collision to be more central, which in turn increases the probability for multiple parton collisions in the event (multiple interactions).

6 Conclusions

We have presented and discussed the most recent results on diffraction from the HERA experiments, H1 and ZEUS. Inclusive diffraction have been shown to be closely related to the high gluon density in the proton. With exclusive processes studies, we have illustrated the importance of t-slope measurements in order to get a better understanding of how quarks and gluons are assembled in the nucleon.

References

[1] K. Golec-Biernat, M. Wüsthoff, Phys. Rev. D **59** (1999) 014017 [hep-ph/9807513].

[2] A. Stasto, K. Golec-Biernat, J. Kwiecinski, Phys. Rev. Lett. **86** (2001) 596 [hep-ph/0007192].

[3] ZEUS Collaboration, Phys. Lett. B **315** (1993) 481;
H1 Collaboration, Nucl. Phys. B **429** (1994) 477.

[4] L. Schoeffel, Prog. Theor. Phys. Suppl. **187** (2011) 179 [arXiv:1010.3553 [hep-ph]].

[5] A. Kaidalov, V. Khoze, A. Martin, M. Ryskin, Eur. Phys. J. C **21** (2001) 521 [hep-ph/0105145].

[6] M. Arneodo, M. Diehl, V. Khoze, P. Newman, proc. of the 2006-8 HERA-LHC Workshop, DESY-PROC-2009-02, 397, and references therein.

[7] H1 Collaboration, Eur. Phys. J. C **48** (2006) 715 [hep-ex/0606004].

[8] H1 Collaboration, Eur. Phys. J. C **48** (2006) 749 [hep-ex/0606003].

[9] ZEUS Collaboration, Nucl. Phys. B **816** (2009) 1 [hep-ex/0812.2003].

[10] H1 Collaboration, *'Measurement of diffractive DIS with a leading proton at HERA-2'* [H1prelim-09-012].

[11] H1 Collaboration, *'Measurement of Inclusive Diffractive DIS at HERA (99-04 data)'* [H1prelim-06-014].

[12] ZEUS Collaboration, Nucl. Phys. B **800** (2008) 1 [hep-ex/0802.3017].

[13] P. Newman, M. Ruspa, proc. of the 2006-8 HERA-LHC Workshop, DESY-PROC-2009-02, 401 [hep-ex/0903.2957].

[14] J. Bartels, J. Ellis, H. Kowalski, M. Wüsthoff, Eur. Phys. J. C **7** (1999) 443 [hep-ph/9803497].

[15] A. Hebecker, T. Teubner, Phys. Lett. B **498** (2001) 16 [hep-ph/0010273].

[16] E. Feinberg, I. Pomeranchuk, Suppl. Nuovo. Cimento. **3** (1956) 652;
V. Gribov, JETP Lett. **41** (1961) 667.

[17] A. Donnachie, P. Landshoff, Phys. Lett. B **296** (1992) 227 [hep-ph/9209205];
J. Cudell, K. Kang, S. Kim, Phys. Lett. B **395** (1997) 311 [hep-ph/9601336].

[18] G. Jaroszkiewicz, P. Landshoff, Phys. Rev. D **10** (1974) 170;
P. Landshoff, Nucl. Phys. Proc. Suppl. **12** (1990) 397.

[19] ZEUS Collaboration, Eur. Phys. J. C **14** (2000) 213 [hep-ex/9910038];
H1 Collaboration, *'Measurement of Pomeron Trajectory in Elastic ρ^0 Photoproduction'* [H1prelim-06-016]

[20] J. Collins, Phys. Rev. D **57** (1998) 3051 [Erratum-ibid. D **61** (2000) 019902] [hep-ph/9709499].

[21] L. Trentadue, G. Veneziano, Phys. Lett. B **323** (1994) 201;
A. Berera, D. Soper, Phys. Rev. D **53** (1996) 6162 [hep-ph/9509239].

[22] G. Ingelman, P. Schlein, Phys. Lett. B **152** (1985) 256;
A. Donnachie, P. Landshoff, Phys. Lett. B **191** (1987) 309 [Erratum-ibid. B **198** (1987) 590].

[23] ZEUS Collaboration, *'A QCD analysis of diffractive DIS data from ZEUS'* [ZEUS-pub-09-010].

[24] R. Thorne, R. Roberts, Phys. Rev. D **57** (1998) 6871 [hep-ph/9709442].

[25] H1 Collaboration, JHEP **0710** (2007) 042 [hep-ex/0708.3217].

[26] L. Schoeffel, Prog. Part. Nucl. Phys. **65** (2010) 9 [arXiv:0908.3287 [hep-ph]].

[27] F. D. Aaron *et al.* [H1 Collaboration], Phys. Lett. B **659** (2008) 796; arXiv:0907.5289 [hep-ex].

[28] S. Chekanov *et al.* [ZEUS Collaboration], JHEP **0905** (2009) 108.

[29] K. Kumericki, D. Mueller and K. Passek-Kumericki, Nucl. Phys. B **794** (2008) 244.

[30] M. Burkardt, Int. J. Mod. Phys. A **18** (2003) 173 [hep-ph/0207047].

[31] M. Diehl, Eur. Phys. J. C **25** (2002) 223 [Erratum-ibid. C **31** (2003) 277] [hep-ph/0205208].